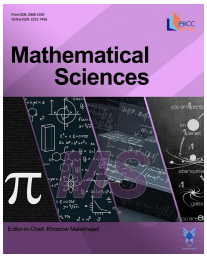

Math. Sci. 2026; 19 (4): 1-20

Mathematical Sciences (MS)

https://doi.org/10.57647/mathsci.2025.1904.17

Original Research

Modeling Fréchet Distribution Using Novel Statistical Family: Mathematical Properties, Simulation Study and Applications in Epidemiological and Environmental Data

Aadil Ahmad Mir[1], Shamshad Ur Rasool[2], M. A. Lone[1], Abdulrahman M. A. Aldawsari[3,*], Abdulmajeed A. R. Alharbi [4]

[1]*Department of Statistics, University of Kashmir, Srinagar 190006, India*
[2]*Department of Statistics, School of Chemical Engineering and Physical Sciences Lovely Professional University, Jalandhar, Punjab, 144411, India*
[3]*Department of Mathematics, College of Sciences and Humanities, Prince Sattam Bin Abdulaziz University, Al-Kharj 16273, Saudi Arabia*
[4]*Department of Statistics and Operations Research, College of Science, King Saud University, P.O.Box 2455, Riyadh 11451, Saudi Arabia*

[*]**Corresponding author:** abd.aldawsari@psau.edu.sa

Received:
21 August 2025
Revised:
17 October 2025
Accepted:
27 October 2025
Published in Issue:
30 December 2025

Abstract:

In this study, we introduce a novel and highly flexible probability model, called the *Novel Exponentiated G-family distribution (NEGFD)*, which serves as a general framework for generating new probability models. We apply this framework to the Fréchet distribution, resulting in the *Novel Exponentiated G-family Fréchet distribution (NEGFFD)*, which extends the classical Fréchet model by incorporating greater flexibility in modeling skewness and tail behavior. Rooted in the broader class of exponentiated G-families, this approach enhances modeling flexibility, making it particularly effective for capturing skewed and heavy-tailed patterns commonly observed in empirical data. Theoretical aspects of the model are rigorously developed, including derivations of its moments, incomplete moments and hazard rate function. To evaluate the performance of parameter estimation, a detailed Monte Carlo simulation study is conducted using the method of maximum likelihood estimation (MLE) under various sample sizes. The simulation findings demonstrate the consistency, efficiency, and robustness of the maximum likelihood estimates (MLEs) across different scenarios. The practical usefulness of the proposed distribution is illustrated through its application to real-world dataset; epidemiological data and environmental data. In both domains, the model exhibits superior performance compared to the classical Fréchet and related competing models, as evidenced by lower values of standard model selection criteria. Additional graphical diagnostics and non-parametric goodness-of-fit assessments further support the proposed model's effectiveness and flexibility in real data modeling contexts.

Keywords: Novel exponentiated G-family; Frechet distribution; Properties; Estimation; Simulation; Epidemiological data; Environmental data

Cite this article: Mir. A.A., Ur Rasool. S., Lone. M.A., Aldawsari A.M.A., Alharbi. A.A.R., Modeling Fréchet Distribution Using Novel Statistical Family: Mathematical Properties, Simulation Study and Applications in Epidemiological and Environmental Data. Math. Sci. 2025; *19* (4): 1-20 https://doi.org/10.57647/mathsci.2025.1904.17

1. Introduction

The statistical modeling of extreme events is a critical endeavor in fields ranging from finance and climatology to engineering and materials science. These domains are often characterized by data with heavy-tailed behavior, where the probability of observing unusually large values is non-negligible. The Generalized Extreme Value distribution provides the foundational asymptotic theory for such maxima, unifying three limit distributions into

a single family: the Gumbel, Fréchet, and Weibull types [1]. Among these, the Fréchet distribution, introduced by Maurice Fréchet in [2], is uniquely suited for modeling data with heavy upper tails and a pronounced positive skew. The Fréchet distribution is a continuous probability distribution widely recognized for its role in modeling extreme events and heavy-tailed phenomena. It belongs to the class of extreme value distributions and is often employed when the underlying data exhibit skewness, high variability, and a propensity for unusually large observations.

The limitations of classical distributions have spurred a vibrant field of research dedicated to developing more flexible generalized families. The core strategy involves embedding a baseline Cumulative Distribution Function (CDF), within a generative structure that introduces new parameters to enhance shape flexibility, improve goodness-of-fit, and provide a better tool for tail-risk analysis. In recent years, the growing complexity of real-world data structures has driven the need for more sophisticated probability distribution models. Classical distributions, though fundamental to statistical theory, frequently fall short in terms of adaptability and precision when applied to complex modern datasets. To address these shortcomings, researchers have introduced various generalized distribution families, which broaden the scope of traditional models and offer improved theoretical understanding along with enhanced applicability across diverse practical scenarios.

One of the earliest development was the exponentiated class, first introduced by Mudholkar and Srivastava [3], provides a fundamental approach to extending existing distributions through CDF transformation given by

$$H(x;\theta,\boldsymbol{\lambda}) = [F_0(x;\boldsymbol{\lambda})]^{\theta}; \quad \theta > 0,\ \boldsymbol{\lambda} > 0,\ x \in \mathbb{R},$$

where $F_0(x;\boldsymbol{\lambda})$ denotes the baseline distribution function characterized by the parameter vector $\boldsymbol{\lambda}$, and θ is an additional shape parameter that governs the distribution's flexibility. This simple transformation adds a new shape parameter that can flexibly model proportional hazards and skewness.

Marshall and Olkin [4] proposed a distinct method for generating new probability models, referred to as the Marshall–Olkin distribution family, which extends existing distributions. The CDF for this class is formulated as:

$$H(x;\delta,\boldsymbol{\eta}) = \frac{F_0(x;\boldsymbol{\eta})}{1-(1-\delta)\left[1-F_0(x;\boldsymbol{\eta})\right]},$$

where $\delta > 0,\ \boldsymbol{\eta} > 0,\ x \in \mathbb{R}$.

Odhah et al. [5] introduced a novel class of probability distributions utilizing trigonometric transformations. This approach captures non-linear behavior and has been shown to provide excellent fits for data with modal characteristics that standard models miss. The CDF for this family is expressed as:

$$H(x;\boldsymbol{\theta}) = \frac{\exp\left(1-\cos\left(\frac{\pi F_0(x;\boldsymbol{\theta})}{1+F_0(x;\boldsymbol{\theta})}\right)\right)-1}{e-1}; \boldsymbol{\theta} > 0,\ x \in \mathbb{R}.$$

Furthermore, Shah et al. [6] developed a more adaptable probability distribution by applying the T-X transformation framework outlined in [7]. This approach resulted in the formulation of the new generalized exponent power X (NGEP-X) family, with its CDF defined as:

$$H(x;\delta,\boldsymbol{\lambda}) = 1-\left(e^{\delta F_0(x;\boldsymbol{\lambda})} - e^{\delta F_0(x;\boldsymbol{\lambda})}\right); \delta \in \mathbb{R}^+,\ x \in \mathbb{R}.$$

Trigonometric transformations have emerged as powerful tools for modifying distributional shapes without increasing the number of parameters. One prominent example is the sine-G family proposed by kumar et al. [8], which employs a sine-based transformation on the CDF of a baseline model. This method improves shape adaptability while maintaining the structural simplicity of the original distribution. The CDF and probability density function (PDF) for the sine-G class are given as:

$$H(x;\boldsymbol{\theta}) = \sin\left(\frac{\pi}{2}F_0(x;\boldsymbol{\theta})\right),$$

$$h(x;\boldsymbol{\theta}) = \frac{\pi}{2}f_0(x;\boldsymbol{\theta})\cos\left(\frac{\pi}{2}F_0(x;\boldsymbol{\theta})\right).$$

In addition to the above, some innovative techniques for generating probability distributions have also been recently proposed by Ahmad et al. [9] and Rasool et al. [10]. In parallel with the development of these general generators, there has been a concerted effort to specifically generalize the Fréchet distribution. Researchers have applied the aforementioned techniques to the Fréchet baseline, yielding models like the include the exponent beta Fr'echet distribution [11], the exponentiated Fr'echet—-Weibull model [12], and size-biased versions [13].

While these generalizations represent significant advancements, a critical review reveals two persistent challenges: Many of these models introduce two or more additional parameters. While this increases flexibility, it often leads to complex estimation procedures, potential identifiability issues, and inflated standard errors—a classic manifestation of the bias-variance trade-off. Some of the simpler one-parameter generators, while parsimonious, may not offer a sufficient degree of shape flexibility, particularly in modifying the central tendency and the lower tail of the distribution simultaneously with the upper tail. There is a need for a generalized Fréchet distribution that strikes an optimal balance between parsimony and flexibility. The proposed *NEGFD* is designed to address this gap directly. Our model is built upon the Novel Exponentiated G-family. This generator was selected because it induces a highly flexible skewness and kurtosis structure while typically adding only a single parameter. Unlike the exponentiated or Marshall-Olkin families, our approach is capable of generating non-monotonic hazard functions, making it suitable for reliability data where the failure rate initially increases and then decreases. Furthermore, compared to existing trigonometric families like the sine-G, our transformation offers a distinct and more adaptable way to modulate both the body and the tail of the baseline

https://doi.org/10.57647/mathsci.2025.1904.17

Fréchet distribution. By unifying the well-established tail behavior of the Fréchet distribution with the innovative shape capabilities of the Novel Exponentiated G-family, we propose a model that is both tractable and exceptionally adaptable. We anticipate it will provide a superior fit for heavy-tailed data in areas like finance and medical science, where accurate estimation of extreme quantiles is paramount, without the computational burden of over-parameterized models. The following sections will detail the formal definition, mathematical properties, and empirical superiority of the proposed distribution

The motivation for generating a family of probability distributions arises from the need to develop models that can flexibly capture diverse and complex data behaviors observed in real-world applications. Here is the motivation for generating a family of distributions:

- Real-world datasets in medicine, environmental, finance, and engineering often display skewness, heavy tails, kurtosis variations, or other complex behaviors that classical probability models cannot adequately capture.
- Traditional distributions usually have a fixed shape, which limits their ability to adapt to diverse data characteristics and reduces model accuracy in empirical studies.
- Generating a family of distributions by introducing one or more shape parameters provides additional flexibility to control tail behavior, peakness, and skewness.
- Such generalized families can unify several existing distributions as special cases, allowing a single modeling framework to address a broad range of data types.
- A family-generating approach also facilitates the construction of models with better goodness-of-fit properties, improving predictive performance and interpretability.
- In applied fields such as lifetime analysis, reliability engineering, hydrology, and risk assessment, having a flexible distribution is crucial to accommodate the variability and complexity of observed data.
- Extending the classical Fréchet distribution through a novel family-generating method enhances its adaptability while preserving its theoretical strengths.
- This methodological advancement enables the development of models capable of capturing extreme events, tail dependencies, and heterogeneous data patterns, making them highly valuable for both theoretical and applied statistics.

The remainder of the paper is organized as follows. Section 2 introduces the NEGFD , outlining its construction. Section 3 defines the NEGFD with baseline model as Fr'echet distribution and presents its main characteristics along with statistical properties. Section 4 focuses on parameter estimation using MLE. Simulation studies validating the proposed estimators are reported in Section 5, and real-data applications are presented in Section 6. Finally, Section 7 summarizes the key findings and outlines promising directions for future research.

2. Novel exponentiated G-family

In this section, we introduce the Novel Exponentiated G-Family. The main motivation for developing this family is to improve the flexibility of existing probability models by adding an extra parameter that modifies the shape and scale characteristics of the baseline distribution. This transformation enhances the modeling capability of the family, making it more suitable for handling complex real-world datasets, particularly in areas such as medical, engineering, finance, and survival analysis.

Let $G(x)$ represents the CDF of the reference model. Then, the CDF $F(x)$ of the NEGFD is obtained as:

$$F(x) = \frac{\alpha(1-\bar{G}^{\alpha}(x))}{\alpha+\bar{\alpha}\bar{G}^{\alpha}(x)}; \quad x>0, \tag{1}$$

where $\alpha>0, \alpha\neq 1, \bar{\alpha}=1-\alpha, \bar{G}(x)=1-G(x)$. In order to determine whether equation (1) is accurate, we must prove the following lemma:

Lemma 1: The CDF $F(x)$ obtained in equation (1) holds in closed form, if

$$\lim_{x\to-\infty} F(x)=0 \quad \text{and} \quad \lim_{x\to\infty} F(x)=1.$$

Proof: We begin by considering the following:

$$\begin{aligned}\lim_{x\to-\infty} F(x) &= \lim_{x\to-\infty} \frac{\alpha(1-\bar{G}^{\alpha}(x))}{\alpha+\bar{\alpha}\bar{G}^{\alpha}(x)} \\ &= \frac{\alpha(1-\bar{G}^{\alpha}(-\infty))}{\alpha+\bar{\alpha}\bar{G}^{\alpha}(-\infty)}=0.\end{aligned}$$

Also,

$$\begin{aligned}\lim_{x\to\infty} F(x) &= \lim_{x\to\infty} \frac{\alpha(1-\bar{G}^{\alpha}(x))}{\alpha+\bar{\alpha}\bar{G}^{\alpha}(x)}, \\ &= \frac{\alpha(1-\bar{G}^{\alpha}(\infty))}{\alpha+\bar{\alpha}\bar{G}^{\alpha}(\infty)}=1. \qquad \square\end{aligned}$$

Property 1: The CDF $F(x)$ derived in equation (1) is right-continuous and differentiable.

$$\frac{d}{dx}F(x)=f(x).$$

Thus, based on lemma 1 and property 1, we have determined that the CDF given in equation (1) is valid. The corresponding PDF of the NEGFD, derived from equation (1) is provided as:

$$f(x)=\frac{\alpha^2\,\bar{G}^{\alpha-1}(x)g(x)}{(\alpha+\bar{\alpha}\bar{G}^{\alpha}(x))^2}. \tag{2}$$

Here, $g(x)=\frac{d}{dx}G(x)$ is the PDF of the reference model and $G(x)$ is the baseline CDF.

https://doi.org/10.57647/mathsci.2025.1904.17

- When $\alpha = 1$, equation (1) reduces to $G(x)$, the CDF of the baseline distribution.

Lemma 2: To confirm that equation (2) defines a valid PDF, it is necessary to verify that

$$\int_{-\infty}^{\infty} f(x)\,dx = 1.$$

Accordingly, we evaluate the integral as follows:

$$\int_{-\infty}^{\infty} f(x)\,dx = \int_{-\infty}^{\infty} \frac{\alpha^2\,\bar{G}^{\alpha-1}(x)g(x)}{(\alpha+\bar{\alpha}\bar{G}^{\alpha}(x))^2}dx.$$

Substituting $\alpha + \bar{\alpha}\bar{G}^{\alpha}(x) = u$, we get

$$\int_{-\infty}^{\infty} f(x)\,dx = -\frac{\alpha}{\bar{\alpha}}\int_{\alpha}^{1}\frac{1}{u^2}\,du = 1.$$

The reliability functions derived from well-known generators, which hold significant importance in probability and related scientific fields, are often expressed in a unified form. These measures are defined as follows: $R(x)$ denotes the reliability function, $h(x)$ represents the hazard rate function, $\Lambda(x)$ denotes the cumulative hazard rate function, and $h_r(x)$ corresponds to the reverse hazard rate function.

The reliability function for NEGFD is obtained as

$$R(x) = \frac{\bar{G}^{\alpha}(x)}{\alpha+\bar{\alpha}\bar{G}^{\alpha}(x)}.$$

The hazard rate for NEGFD is obtained as

$$h(x) = \frac{\alpha^2 g(x)}{\bar{G}(x)(\alpha+\bar{\alpha}\bar{G}^{\alpha}(x))}.$$

The reversed hazard rate for NEGFD is obtained as

$$h_r(x) = \frac{\alpha\bar{G}^{\alpha-1}(x)g(x)}{(1-\bar{G}^{\alpha}(x))(\alpha+\bar{\alpha}\bar{G}^{\alpha}(x))}.$$

The cumulative hazard rate for NEGFD is obtained for NEGFD as

$$\Lambda(x) = \frac{\alpha+\bar{\alpha}\bar{G}^{\alpha}(x)}{\bar{G}^{\alpha}(x)}.$$

For the NEGFD, the inversion of $F(x)$ is required to derive the quantile function $G_X(u)$. Thus, the quantile function of the NEGFD is expressed as

$$x = G^{-1}\left\{1-\left(\frac{(1-u)\alpha}{u\bar{\alpha}+\alpha}\right)^{\frac{1}{\alpha}}\right\}; \quad 0<u<1.$$

Given a baseline CDF, random samples from the NEGFD can be generated using equation (2).

3. Novel exponentiated G-family Fréchet distribution and its properties

The Novel Exponentiated G-Family Fréchet Distribution (NEGFFD) is a new flexible probability distribution proposed and analysed in this section. It is constructed within the framework of the Novel Exponentiated G-Family (NEGFD) by employing the Fréchet distribution as the baseline model. The incorporation of an additional shape parameter through the NEGFD generator substantially enhances the flexibility of the classical Fréchet distribution, enabling it to accommodate a wide range of data behaviours, including skewness, heavy tails. The proposed model, characterised by three parameters (α, β, θ), provides an analytically tractable approach for modelling a wide range of lifetime and reliability patterns observed in real-world data. In this section, we derive and analyse several key statistical and structural properties of the NEGFFD, including its PDF, CDF, reliability function, hazard rate function, inverse hazard rate function, and cumulative hazard rate function. Additional analytical developments include the quantile function, PDF expansion, moments and moment-generating function, incomplete moments, Lorenz and Bonferroni inequality curves, mean residual life (MRL), mean waiting time (MWT), entropy measures such as Rényi and Tsallis entropies, and order statistics. These comprehensive derivations demonstrate the analytical tractability and mathematical robustness of the NEGFFD, as well as its potential applicability across a wide range of statistical contexts.

The Fréchet distribution has the following CDF:

$$G(x) = e^{-\left(\frac{\beta}{x}\right)^{\theta}}; \quad x>0, \quad \theta,\beta>0.$$

The corresponding PDF of Fréchet distribution is defined as

$$g(x) = \theta\beta^{\theta}x^{-\theta-1}e^{-\left(\frac{\beta}{x}\right)^{\theta}}; \quad x>0, \quad \theta,\beta>0, \quad (3)$$

where β and θ are scale and shape parameters, respectively. Survival function for Fréchet distribution is given by

$$\bar{G}(x) = 1-e^{-\left(\frac{\beta}{x}\right)^{\theta}}; \quad x>0, \quad \theta,\beta>0. \quad (4)$$

By substituting equation (3) into equation (1), the CDF of the NEGFFD is obtained, as given by:

$$F(x) = \frac{\alpha\left(1-\left(1-e^{-\left(\frac{\beta}{x}\right)^{\theta}}\right)^{\alpha}\right)}{\alpha+\bar{\alpha}\left(1-e^{-\left(\frac{\beta}{x}\right)^{\theta}}\right)^{\alpha}}; \quad x>0, \quad \alpha,\beta,\theta>0, \quad (5)$$

where $\bar{\alpha} = 1-\alpha$. The corresponding PDF of NEGFFD is given by

$$f(x) = \frac{\alpha^2\theta\beta^{\theta}x^{-\theta-1}\quad e^{-\left(\frac{\beta}{x}\right)^{\theta}}\left(1-e^{-\left(\frac{\beta}{x}\right)^{\theta}}\right)^{\alpha-1}}{\left(\alpha+\bar{\alpha}\left(1-e^{-\left(\frac{\beta}{x}\right)^{\theta}}\right)^{\alpha}\right)^2}, \quad (6)$$

where $x>0, \quad \alpha,\beta,\theta>0, \quad \bar{\alpha}=1-\alpha$.

Fig. 1 illustrates the density functions of the NEGFFD under varying parameter configurations of α, β, and θ.

https://doi.org/10.57647/mathsci.2025.1904.17

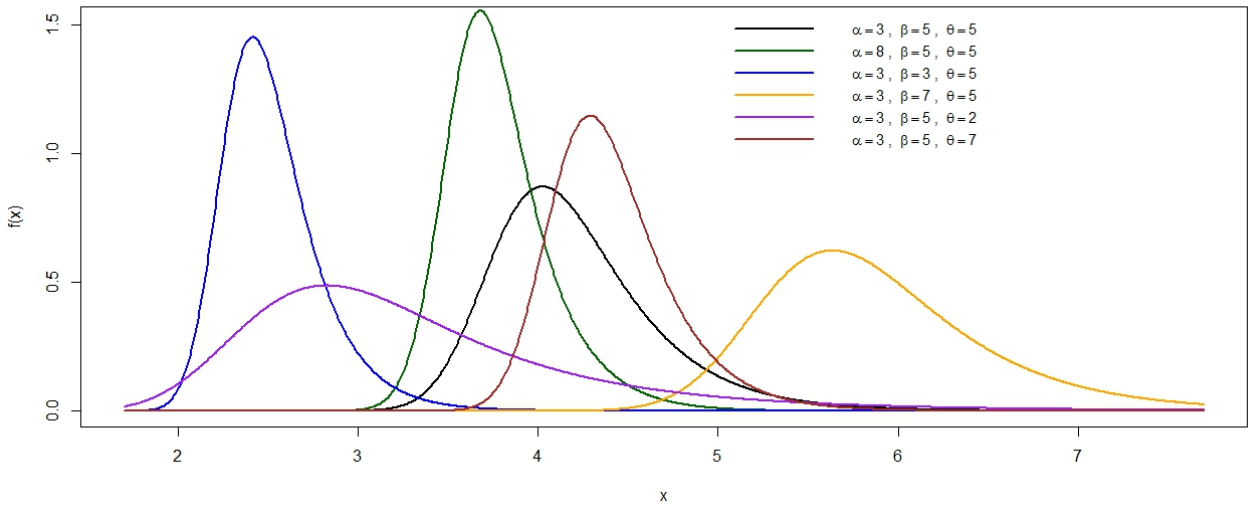

Figure 1. Plots of the NEGFFD density for different values of α, β and θ.

The plots demonstrate the distribution's flexibility in modeling diverse failure rate behaviors. Notably, increasing values of α tend to shift the density peak to the right, indicating a longer initial failure-free period. The scale parameter β influences the spread of the distribution, with higher values resulting in broader and flatter curves. Meanwhile, variations in the shape parameter θ significantly affect the tail behavior, where larger θ values correspond to heavier tails, suggesting an increased probability of late-occurring failures. The interplay between these parameters highlights the NEGFFD's capability to capture complex lifetime data patterns, making it suitable for reliability analysis and risk assessment applications. The distinct curves emphasize the importance of parameter selection in accurately modeling real-world failure processes.

For a low value of $\alpha = 1$, the PDF exhibits a highly right-skewed, J-shaped form, characterized by a sharp peak near the origin and a long, heavy tail. This signifies a high propensity for observations to cluster near very small values, while still allowing for a substantial probability of extremely large values. As α is increased, a consistent trend is observed: the mode of the distribution shifts progressively to the right, the peak of the density becomes simultaneously higher and narrower, and the tail of the distribution decays more rapidly. This progression indicates that increasing α leads to a greater concentration of probability mass around a central value, effectively reducing both the skewness and the kurtosis of the distribution.

The reliability function is defined as the probability that the system will continue to function beyond a specified time t and is obtained for NEGFFD as

$$R(x) = \frac{\left(1 - e^{-\left(\frac{\beta}{x}\right)^{\theta}}\right)^{\alpha}}{\alpha + \bar{\alpha}\left(1 - e^{-\left(\frac{\beta}{x}\right)^{\theta}}\right)^{\alpha}}. \tag{7}$$

The hazard rate, often referred to as the failure rate, represents the instantaneous risk of failure at a specific time, conditional on the fact that the subject has survived up to that time. It provides useful insights into the likelihood of failure as time progresses. Hazard rate for NEGFFD is given by

$$h(x) = \frac{\alpha^2\theta\beta^{\theta}x^{-\theta-1}e^{-\left(\frac{\beta}{x}\right)^{\theta}}}{\left(1 - e^{-\left(\frac{\beta}{x}\right)^{\theta}}\right)\left(\alpha + \bar{\alpha}\left(1 - e^{-\left(\frac{\beta}{x}\right)^{\theta}}\right)^{\alpha}\right)}.$$

The hazard rate function, denoted by $h(x)$, represents the instantaneous rate of failure at any given time x, conditional on survival up to that time. It provides valuable insights into the failure mechanism and the reliability characteristics of a system or component. Figure 3 illustrates the hazard rate behavior of the NEGFFD under different parameter combinations of (α, β, θ).

The graphical behavior demonstrates that the NEGFFD is capable of exhibiting a wide range of hazard rate shapes depending on the parameter values. For instance, when $(\alpha = 5, \beta = 2, \theta = 5)$, the hazard rate shows a decreasing trend, indicating a high initial risk that declines over time, which is typical of early-life failures or the infant mortality phase. When $(\alpha = 5, \beta = 5, \theta = 10)$, the hazard function follows a unimodal pattern, where the risk increases initially, reaches a peak, and then decreases, representing a wear-in and wear-out failure mechanism. For $(\alpha = 4, \beta = 3, \theta = 7)$, the hazard curve displays a sharp initial peak followed by a rapid decline, corresponding to systems with early peak failures and short operational lifetimes.

In the case of $(\alpha = 20, \beta = 6, \theta = 4)$, the hazard rate gradually increases, attains a maximum, and then declines, indicating a system that experiences a maturity phase before degradation. The parameter set $(\alpha = 12, \beta = 7, \theta = 4)$ exhibits an initially increasing

https://doi.org/10.57647/mathsci.2025.1904.17

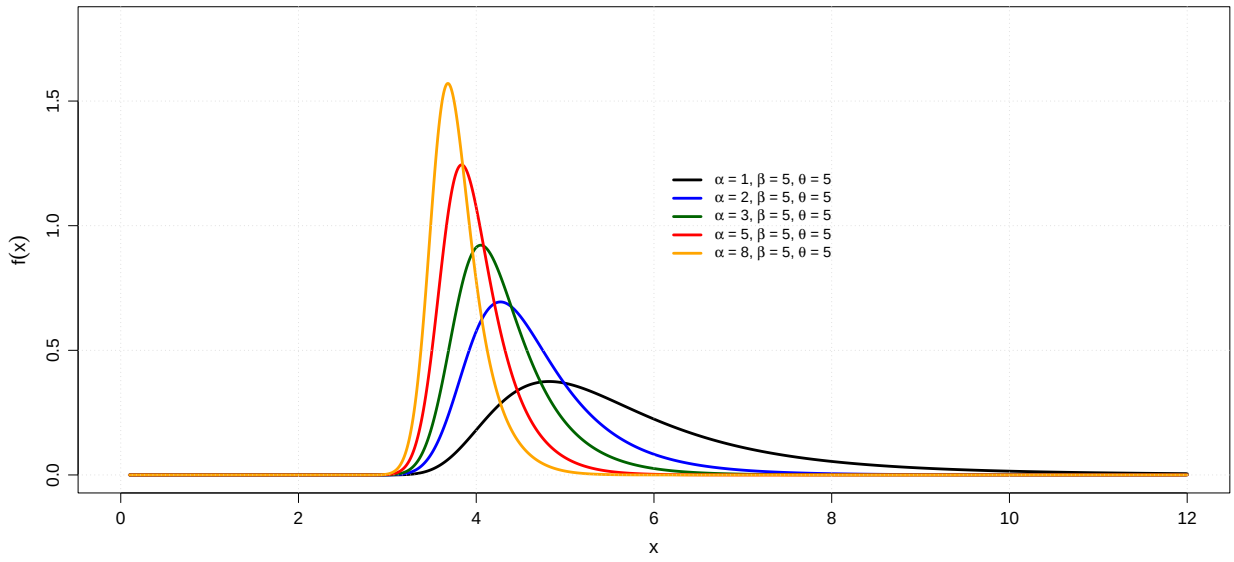

Figure 2. Plots of the NEGFFD density for different values of α, keeping β and θ fixed.

and then flattening hazard pattern, followed by a decrease, which reflects a bathtub-shaped hazard function commonly observed in reliability data, characterized by early failures, a steady operational phase, and eventual wear-out failures.

Overall, the NEGFFD demonstrates remarkable flexibility in modeling diverse hazard rate behaviors such as decreasing, increasing, unimodal, and bathtub-shaped patterns. This flexibility enhances its applicability in various practical contexts, including reliability analysis of mechanical and electronic systems, and survival studies in biomedical research. The ability of the NEGFFD to accommodate such diverse failure mechanisms makes it a powerful and versatile model for analyzing lifetime data.

The reverse hazard rate function describes the likelihood of failure occurring at a specific time, given that the event has not occurred earlier. Formally, it is defined as the ratio of the probability density function to the cumulative distribution function, and is widely applied in reliability analysis and lifetime modeling.

Reversed hazard rate for NEGFFD is given by

$$h_r(x) = \frac{\alpha\theta\beta^\theta x^{-\theta-1} e^{-\left(\frac{\beta}{x}\right)^\theta}\left(1-e^{-\left(\frac{\beta}{x}\right)^\theta}\right)^{\alpha-1}}{\left(1-\left(1-e^{-\left(\frac{\beta}{x}\right)^\theta}\right)^\alpha\right)\left(\alpha+\bar{\alpha}\left(1-e^{-\left(\frac{\beta}{x}\right)^\theta}\right)^\alpha\right)}.$$

The cumulative hazard rate is obtained by integrating the hazard rate over time, and it reflects the total risk of failure accumulated up to a given time point and is obtained for NEGFFD as

$$\Lambda(x) = \frac{\alpha+\bar{\alpha}\left(1-e^{-\left(\frac{\beta}{x}\right)^\theta}\right)^\alpha}{\left(1-e^{-\left(\frac{\beta}{x}\right)^\theta}\right)^\alpha}.$$

The quantile function plays a crucial role in characterizing the random variable of a distribution. It is particularly useful for generating random samples in simulation studies and for deriving various statistical measures, including (but not limited to) skewness and kurtosis. Quantile function for NEGFFD is given by

$$x = \frac{\beta}{\left[-log\left\{1-\left(\frac{(1-u)\alpha}{u\bar{\alpha}+\alpha}\right)^{\frac{1}{\alpha}}\right\}\right]^{\frac{1}{\theta}}}.$$

3.1 Expansion form

The PDF of equation (6) can be written as

$$f(x) = \frac{\theta\beta^\theta x^{-\theta-1} \quad e^{-\left(\frac{\beta}{x}\right)^\theta}\left(1-e^{-\left(\frac{\beta}{x}\right)^\theta}\right)^{\alpha-1}}{\left(1+\frac{\bar{\alpha}}{\alpha}\left(1-e^{-\left(\frac{\beta}{x}\right)^\theta}\right)^\alpha\right)^2}.$$

Using expansion form

$$(1+x)^{-2} = \sum_{k=0}^{\infty}(-1)^k(k+1)x^k; \qquad |x|<1.$$

We get

$$\begin{aligned} f(x) &= \theta\beta^\theta \sum_{k=0}^{\infty}(-1)^k(k+1)\left(\frac{\bar{\alpha}}{\alpha}\right)^k x^{-\theta-1} \\ &\quad \times e^{-\left(\frac{\beta}{x}\right)^\theta}\left(1-e^{-\left(\frac{\beta}{x}\right)^\theta}\right)^{\alpha(k+1)-1}. \end{aligned}$$

Again using expansion form

$$(1-x)^j = \sum_{p=0}^{\infty}(-1)^p\binom{j}{p}x^p.$$

https://doi.org/10.57647/mathsci.2025.1904.17

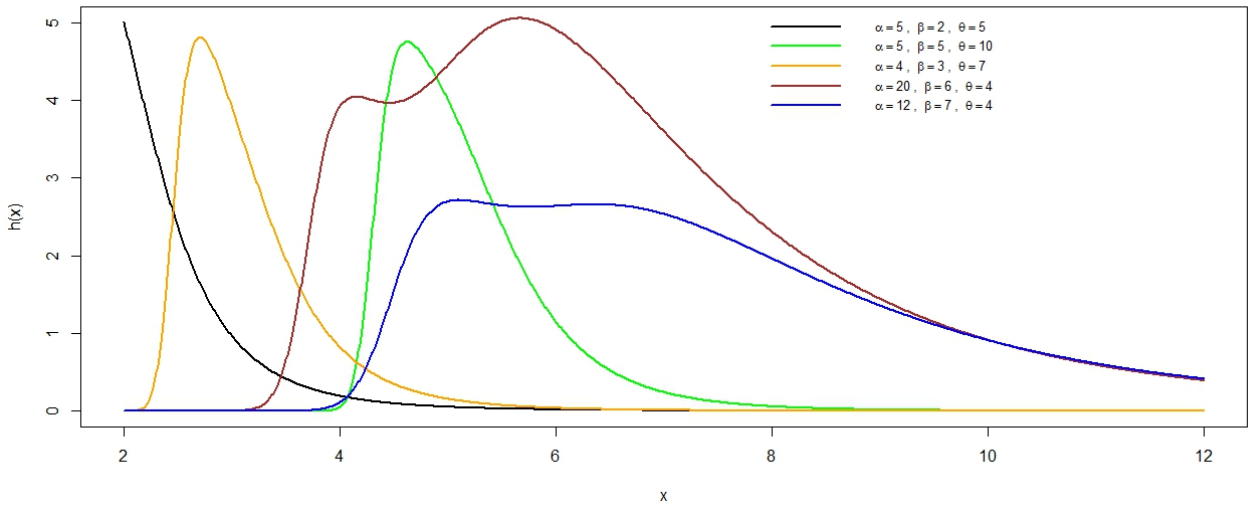

Figure 3. Plots of the NEGFFD hazard rate function for different values of α, β and θ.

We get PDF of NEGFFD in expansion form as given by

$$f(x) = \theta\beta^{\theta}\sum_{k=0}^{\infty}\sum_{p=0}^{\infty}(-1)^{k+p}(k+1)\left(\frac{\bar{\alpha}}{\alpha}\right)^{k} \times\binom{\alpha(k+1)-1}{p}x^{-\theta-1}e^{-(p+1)\left(\frac{\beta}{x}\right)^{\theta}}. \quad (8)$$

3.2 Moments and moment generating function

Moments are key statistical measures that capture important characteristics of a probability distribution, including its location, spread, skewness, and kurtosis. Moments are calculated not only to describe the shape and variability of the distribution, but also to serve as a foundation for deriving other important properties, including the mean residual life , mean waiting time and entropy. Hence, they provide both descriptive and analytical insights into the behavior of the distribution.

For the NEGFFD, the ordinary r^{th} moment is calculated as

$$\mu_r{}' = \int_0^{\infty} x^r f(x)dx. \quad (9)$$

Substituting equation (8) in equation (9), we get

$$\mu_r{}' = \theta\beta^{\theta}\sum_{k=0}^{\infty}\sum_{p=0}^{\infty}(-1)^{k+p}(k+1)\left(\frac{\bar{\alpha}}{\alpha}\right)^{k} \times\binom{\alpha(k+1)-1}{p}\int_0^{\infty}x^{r-\theta-1}e^{-(p+1)\left(\frac{\beta}{x}\right)^{\theta}}dx.$$

On substituting $(p+1)\left(\frac{\beta}{x}\right)^{\theta} = z$, we get r^{th} moment of NEGFFD as given by

$$\mu_r{}' = \beta^r\sum_{k=0}^{\infty}\sum_{p=0}^{\infty}(-1)^{k+p}(k+1)(p+1)^{\frac{r-\theta}{\theta}}\left(\frac{\bar{\alpha}}{\alpha}\right)^{k} \times\binom{\alpha(k+1)-1}{p}\Gamma(1-\frac{r}{\theta}). \quad (10)$$

Put $r = 1$, in equation (10) the mean of the NEGFFD is computed as

$$\mu_1{}' = \beta^r\sum_{k=0}^{\infty}\sum_{p=0}^{\infty}(-1)^{k+p}(k+1)(p+1)^{\frac{1-\theta}{\theta}}\left(\frac{\bar{\alpha}}{\alpha}\right)^{k} \times\binom{\alpha(k+1)-1}{p}\Gamma(1-\frac{1}{\theta}). \quad (11)$$

Similarly for $r = 2$, 3 and 4 in equation (10) ,the second, third and fourth moment about origin are respectively.

Using the series representation of e^{tx}, we have

$$M_X(t) = \sum_{r=0}^{\infty}\frac{t^r}{r!}E(X^r). \quad (12)$$

Substituting the value of equation (10) in equation (12), we get Moment Generating Function of NEGFFD as:

$$M_X(t) = \sum_{k=0}^{\infty}\sum_{p=0}^{\infty}\sum_{r=0}^{\infty}\frac{t^r}{r!}\beta^r\left(\frac{\bar{\alpha}}{\alpha}\right)^{k}(p+1)^{\frac{r-\theta}{\theta}}(-1)^{k+p} \times(k+1)\binom{\alpha(k+1)-1}{p}\Gamma(1-\frac{r}{\theta}).$$

3.3 r^{th} incomplete moment

The incomplete moment describes the contribution of a random variable up to a truncation point t, and is particularly useful in studying reliability characteristics and inequality measures.

The r^{th} incomplete moment is defined as

$$\Delta_r(z) = \int_0^{z} x^r f(x)dx. \quad (13)$$

Substituting equation (8) in equation (13), then the r^{th}

https://doi.org/10.57647/mathsci.2025.1904.17

incomplete moment of NEGFFD model is given by

$$\Delta_r(z) = \beta^r \sum_{k=0}^{\infty}\sum_{p=0}^{\infty}(-1)^{k+p}(k+1)(p+1)^{\frac{r-\theta}{\theta}}\left(\frac{\bar{\alpha}}{\alpha}\right)^k \times\binom{\alpha(k+1)}{p}\Gamma\left(\frac{\theta-r}{\theta},\,(p+1)\left(\frac{\beta}{z}\right)^{\theta}\right). \quad (14)$$

Putting $r = 1$ in equation (14), we get the first incomplete moment as given by

$$\Delta_1(z) = \beta\sum_{k=0}^{\infty}\sum_{p=0}^{\infty}(-1)^{k+p}(k+1)(p+1)^{\frac{1-\theta}{\theta}}\left(\frac{\bar{\alpha}}{\alpha}\right)^k \times\binom{\alpha(k+1)}{p}\Gamma\left(\frac{\theta-1}{\theta},\,(p+1)\left(\frac{\beta}{z}\right)^{\theta}\right) \quad (15)$$

3.4 Lorenz and Bonferroni inequality curves

The Bonferroni and Lorenz curves, although originally developed for economic and poverty analysis, have broader applications in various fields. They are frequently used in reliability engineering, lifetime data analysis, insurance, and medical research to study the distribution and inequality of resources, lifetimes, or risks within a population. For a given probability distribution, they are defined by

$$L_p = \frac{1}{E(X)}\int_0^t x f(x)\,dx = \frac{\Delta_1(t)}{E(X)}. \quad (16)$$

Substituting equation (11) and equation (15) into equation (16), we get the following:

$$L_p = \frac{\sum_{k=0}^{\infty}\sum_{p=0}^{\infty}(-1)^{k+p}(k+1)\binom{\alpha(k+1)}{p}\Gamma\left(\frac{\theta-1}{\theta},\,(p+1)\left(\frac{\beta}{t}\right)^{\theta}\right)}{\sum_{k=0}^{\infty}\sum_{p=0}^{\infty}(-1)^{k+p}(k+1)\binom{\alpha(k+1)-1}{p}}.$$

Similarly,

$$B_p = \frac{1}{pE(X)}\int_0^t x f(x)\,dx = \frac{\Delta_1(t)}{pE(X)},$$

$$B_p = \frac{\sum_{k=0}^{\infty}\sum_{p=0}^{\infty}(-1)^{k+p}(k+1)\binom{\alpha(k+1)}{p}\Gamma\left(\frac{\theta-1}{\theta},\,(p+1)\left(\frac{\beta}{t}\right)^{\theta}\right)}{p\sum_{k=0}^{\infty}\sum_{p=0}^{\infty}(-1)^{k+p}(k+1)\binom{\alpha(k+1)-1}{p}}.$$

3.5 Mean residual life (MRL) and mean waiting time (MWT)

For a system component that has survived up to time $t > 0$, the *residual life* represents the remaining time until failure, expressed as the conditional random variable $X - t \mid X > t$. The MRL is an important measure in survival analysis and reliability theory, as it characterizes the expected remaining lifetime of the system and can uniquely determine the associated lifetime distribution.

The MRL is defined as

$$\mu(t) = \frac{1}{R(t)}\left[E(t) - \int_0^t x f(x)\,dx\right] - t = \frac{1}{R(t)}\left[E(t) - \Delta_1(t)\right] - t.$$

After inserting the value of equation (2), (11) and (15), we obtain the required expression for MRL as

$$\mu(t) = \frac{\alpha + \bar{\alpha}\left(1 - e^{-\left(\frac{\beta}{t}\right)^{\theta}}\right)^{\alpha}}{\left(1 - e^{-\left(\frac{\beta}{t}\right)^{\theta}}\right)^{\alpha}}\left[\beta\sum_{k=0}^{\infty}\sum_{p=0}^{\infty}(-1)^{k+p}(k+1) \times\left(\frac{\bar{\alpha}}{\alpha}\right)^k\binom{\alpha(k+1)-1}{p} \times\left(\Gamma\left(1-\frac{1}{\theta}\right) - \Gamma\left(\frac{\theta-1}{\theta},\,(p+1)\left(\frac{\beta}{t}\right)^{\theta}\right)\right)\right] - t.$$

The MWT represents the expected time elapsed until failure, given that the failure occurs within the interval $[0, t]$. It provides insight into the timing of events over a specified period and is used in reliability analysis and queueing theory. The MWT is defined as

$$\overline{\mu}(t) = t - \frac{1}{F(t)}\int_0^t x f(x)\,dx = t - \frac{\Delta_1(t)}{F(t)}.$$

After substituting the value of equations (5) and (15), we obtain the required expression for MWT as

$$\overline{\mu}(t) = t - \frac{\alpha\beta\left(1 - \left(1 - e^{-\left(\frac{\beta}{t}\right)^{\theta}}\right)^{\alpha}\right)}{\alpha + \bar{\alpha}\left(1 - e^{-\left(\frac{\beta}{t}\right)^{\theta}}\right)^{\alpha}} \times\sum_{k=0}^{\infty}\sum_{p=0}^{\infty}(-1)^{k+p}(k+1)\left(\frac{\bar{\alpha}}{\alpha}\right)^k(p+1)^{\frac{1-\theta}{\theta}} \times\binom{\alpha(k+1)-1}{p}\Gamma\left(\frac{\theta-1}{\theta},\,(p+1)\left(\frac{\beta}{t}\right)^{\theta}\right).$$

3.6 Rényi entropy

Entropy quantifies the average uncertainty or information content associated with a random variable. Specifically, the Rényi entropy, introduced by Alfred Rényi [14], generalizes Shannon's classical measure of information and provides a flexible framework to capture the diversity or unpredictability of a distribution. It is widely used to study the randomness, complexity, and information-theoretic properties of probability distributions. The Rényi entropy of order ϕ for the NEGFFD model is defined as

$$R_\phi = \frac{1}{1-\phi}\log\left[\int_0^{\infty} f(x)^{\phi}\,dx\right];\ \phi > 0,\ \phi \neq 1,\ x \in \mathbb{R}. \quad (17)$$

By substituting the expression of $f(x)$ from equation (8) into equation (17), the Rényi entropy of order ϕ for the NEGFFD model becomes

$$R_\phi = \frac{1}{1-\phi}\theta^{\phi-1}\beta^{\phi-\theta} \times\left(\sum_{k=0}^{\infty}\sum_{p=0}^{\infty}(-1)^{k+p}(k+1)\left(\frac{\bar{\alpha}}{\alpha}\right)^k\binom{\alpha(k+1)-1}{p}\right)^{\phi} \times\Gamma\left(\frac{\theta-\phi}{\theta}\right).$$

https://doi.org/10.57647/mathsci.2025.1904.17

3.7 Tsallis q-entropy

The Tsallis entropy, or q-entropy, generalizes Shannon entropy and is particularly useful for systems with non-extensive behavior or long-range correlations. Unlike Shannon or Rényi entropy, it is non-additive, allowing it to capture complex dependencies.

For the NEGFFD model, using the expansion in equation (8), is given by

$$\begin{aligned} Q_\phi &= \frac{1}{\phi-1}\left[1-\theta^{\phi-1}\beta^{\phi-\theta}\right. \\ &\times\left(\sum_{k=0}^{\infty}\sum_{p=0}^{\infty}(-1)^{k+p}(k+1)\right. \\ &\left.\left.\times\left(\frac{\bar{\alpha}}{\alpha}\right)^k\binom{\alpha(k+1)-1}{p}\right)^{\phi}\Gamma\left(\frac{\theta-\phi}{\theta}\right)\right], \end{aligned}$$

where $\phi > 0,\ \phi \neq 1$.

3.8 Order statistics

Order statistics examine the characteristics and behavior of ordered random variables and functions derived from them. These concepts are especially important for analyzing natural and engineering phenomena, such as flood levels, lifespans, material strength, and atmospheric variables, including temperature, pressure, and wind speed. A thorough understanding of extreme observations is essential for predicting the occurrence of rare or critical events, which motivates detailed studies of such extremes.

Suppose $X_1, X_2, \ldots, X_n$ are independent and identically distributed random variables with the PDF and CDF given, respectively, in equations (6) and (5). Then, the pdf and cdf of the m^{th} order statistic, denoted by $f_{X_{(m:n)}}(x)$ and $F_{X_{(m:n)}}(x)$, are given by

$$\begin{aligned} f_{X_{(m:n)}}(x) &= \frac{n!}{(m-1)!(n-m)!}f(x)[F(x)]^{m-1} \\ &\times[1-F(x)]^{n-m}, \end{aligned} \tag{18}$$

and

$$F_{X_{(m:n)}}(x) = \sum_{j=m}^{n}\binom{n}{j}[F(x)]^j\,[1-F(x)]^{n-j}. \tag{19}$$

Substituting equations (6) and (5) into equation (18), we obtain

$$\begin{aligned} f_{X_{(m:n)}}(x) &= \frac{n!}{(m-1)!(n-m)!} \\ &\times\frac{\alpha^2\theta\beta^\theta x^{-\theta-1}e^{-\left(\frac{\beta}{x}\right)^\theta}\left(1-e^{-\left(\frac{\beta}{x}\right)^\theta}\right)^{\alpha-1}}{\left(\alpha+\bar{\alpha}\left(1-e^{-\left(\frac{\beta}{x}\right)^\theta}\right)^{\alpha}\right)^2} \\ &\times\left[\frac{\alpha\left(1-\left(1-e^{-\left(\frac{\beta}{x}\right)^\theta}\right)^{\alpha}\right)}{\alpha+\bar{\alpha}\left(1-e^{-\left(\frac{\beta}{x}\right)^\theta}\right)^{\alpha}}\right]^{m-1} \\ &\times\left[\frac{\left(1-e^{-\left(\frac{\beta}{x}\right)^\theta}\right)^{\alpha}}{\alpha+\bar{\alpha}\left(1-e^{-\left(\frac{\beta}{x}\right)^\theta}\right)^{\alpha}}\right]^{n-m}. \end{aligned}$$

Similarly, substituting into equation (19) yields

$$\begin{aligned} F_{X_{(m:n)}}(x) &= \sum_{j=m}^{n}\binom{n}{j}\left[\frac{\alpha\left(1-\left(1-e^{-\left(\frac{\beta}{x}\right)^\theta}\right)^{\alpha}\right)}{\alpha+\bar{\alpha}\left(1-e^{-\left(\frac{\beta}{x}\right)^\theta}\right)^{\alpha}}\right]^j \\ &\times\left[\frac{\left(1-e^{-\left(\frac{\beta}{x}\right)^\theta}\right)^{\alpha}}{\alpha+\bar{\alpha}\left(1-e^{-\left(\frac{\beta}{x}\right)^\theta}\right)^{\alpha}}\right]^{n-j}. \end{aligned}$$

Hence, these expressions represent the PDF and CDF of the m^{th} order statistic for the NEGFFD model.

4. Estimation approach

This section presents the MLE method for estimating the unknown parameters of the NEGFFD model. Let the random variables $X_1, X_2, ..., X_n$ be a random sample from the NEGFFD model with PDF $f(x;\alpha,\beta,\theta)$ as given in equation (6). The likelihood function corresponding to $f(x;\alpha,\beta,\theta)$, say $L(\alpha,\beta,\theta)$, is given as

$$L(x;\alpha,\beta,\theta) = \prod_{k=1}^{n}\frac{\alpha^2\theta\beta^\theta x_k^{-\theta-1}e^{-\left(\frac{\beta}{x_k}\right)^\theta}\left(1-e^{-\left(\frac{\beta}{x_k}\right)^\theta}\right)^{\alpha-1}}{\left(\alpha+\bar{\alpha}\left(1-e^{-\left(\frac{\beta}{x_k}\right)^\theta}\right)^{\alpha}\right)^2}.$$

Now, the logarithmic likelihood function, say $\ell(x;\alpha,\beta,\theta)$ is given as

$$\begin{aligned} \ell(x;\alpha,\beta,\theta) &= 2n\ln(\alpha)+n\ln(\theta)+n\theta\ln(\beta) \\ &-(\theta+1)\sum_{k=1}^{n}\ln x_k-\sum_{k=1}^{n}\left(\frac{\beta}{x_k}\right)^\theta \\ &+(\alpha-1)\sum_{k=1}^{n}\ln\left(1-e^{-\left(\frac{\beta}{x_k}\right)^\theta}\right) \\ &-2\sum_{k=1}^{n}\ln\left[\alpha+\bar{\alpha}\left(1-e^{-\left(\frac{\beta}{x_k}\right)^\theta}\right)^{\alpha}\right]. \end{aligned}$$

The derivatives of $\ell(x;\alpha,\beta,\theta)$ w.r.to α, β and θ are calculated as:

$$\frac{\partial}{\partial\alpha}\ell(x;\alpha,\beta,\theta) = \frac{2n}{\alpha} + \sum_{k=1}^{n}\ln\left(1-e^{-\left(\frac{\beta}{x_k}\right)^{\theta}}\right) - 2\sum_{k=1}^{n}\frac{1}{\alpha+\bar{\alpha}\left(1-e^{-\left(\frac{\beta}{x_k}\right)^{\theta}}\right)^{\alpha}} \times\left[1+\bar{\alpha}\left(1-e^{-\left(\frac{\beta}{x_k}\right)^{\theta}}\right)^{\alpha}\ln\left(1-e^{-\left(\frac{\beta}{x_k}\right)^{\theta}}\right) - \left(1-e^{-\left(\frac{\beta}{x_k}\right)^{\theta}}\right)^{\alpha}\right],$$

$$\frac{\partial}{\partial\beta}\ell(x;\alpha,\beta,\theta) = \frac{n\theta}{\beta} - \sum_{k=1}^{n}\frac{\theta\beta^{\theta-1}}{x_k^{\theta}} - 2\sum_{k=1}^{n}\frac{\alpha\bar{\alpha}\theta\beta^{\theta-1}\left(1-e^{-\left(\frac{\beta}{x_k}\right)^{\theta}}\right)^{\alpha-1}e^{-\left(\frac{\beta}{x_k}\right)^{\theta}}}{\alpha+\bar{\alpha}\left(1-e^{-\left(\frac{\beta}{x_k}\right)^{\theta}}\right)^{\alpha}}\frac{1}{x_k^{\theta}} + (\alpha-1)\sum_{k=1}^{n}\frac{\theta\beta^{\theta-1}e^{-\left(\frac{\beta}{x_k}\right)^{\theta}}}{x_k^{\theta}}\frac{1}{1-e^{-\left(\frac{\beta}{x_k}\right)^{\theta}}},$$

$$\frac{\partial}{\partial\theta}\ell(x;\alpha,\beta,\theta) = \frac{n}{\theta} + n\ln(\beta) - \sum_{k=1}^{n}\ln x_k - \sum_{k=1}^{n}\left(\frac{\beta}{x_k}\right)^{\theta}\ln\left(\frac{\beta}{x_k}\right) + (\alpha-1)\sum_{k=1}^{n}\frac{\left(\frac{\beta}{x_k}\right)^{\theta}\ln\left(\frac{\beta}{x_k}\right)e^{-\left(\frac{\beta}{x_k}\right)^{\theta}}}{1-e^{-\left(\frac{\beta}{x_k}\right)^{\theta}}} - 2\sum_{k=1}^{n}\frac{\bar{\alpha}\alpha\left(1-e^{-\left(\frac{\beta}{x_k}\right)^{\theta}}\right)^{\alpha-1}e^{-\left(\frac{\beta}{x_k}\right)^{\theta}}\left(\frac{\beta}{x_k}\right)^{\theta}\ln\left(\frac{\beta}{x_k}\right)}{\alpha+\bar{\alpha}\left(1-e^{-\left(\frac{\beta}{x_k}\right)^{\theta}}\right)^{\alpha}}.$$

To obtain the MLEs of α, β and θ, we solve the nonlinear system: $\frac{\partial}{\partial\alpha}\ell(\alpha,\beta,\theta)=0$, $\frac{\partial}{\partial\beta}\ell(\alpha,\beta,\theta)=0$ and $\frac{\partial}{\partial\theta}\ell(\alpha,\beta,\theta)=0$. These equations are typically solved numerically using iterative methods such as the Newton–Raphson algorithm.

5. Simulation study

The simulation study was conducted using R software to examine the behavior of the MLEs with respect to the sample size. Samples of sizes $n = 25, 50, 100, 200$ were generated, each repeated 2000 times for the following four parameter sets:

- Combination 1: $\alpha_0 = 0.5, \beta_0 = 0.5, \theta_0 = 1$
- Combination 2: $\alpha_0 = 1.5, \beta_0 = 0.5, \theta_0 = 1$
- Combination 3: $\alpha_0 = 0.5, \beta_0 = 0.5, \theta_0 = 2$
- Combination 4: $\alpha_0 = 3, \beta_0 = 5, \theta_0 = 2$
- Combination 5: $\alpha_0 = 3, \beta_0 = 1.5, \theta_0 = 2$

For each scenario, the average values of the MLEs along with the corresponding empirical mean squared errors (MSEs) were computed. The results are summarized in Table 1. It is evident from the table that the estimated parameters remain reasonably stable and consistently close to their respective true values across all sample sizes and combinations. Moreover, the MSEs decrease as the sample size increases, indicating that the accuracy of the estimators improves with larger samples. These findings confirm the reliability of the MLEs for estimating the parameters of the NEGFFD distribution under the chosen settings. Figs. 4, 5, 6, 7 and 8 present the graphical representation of the MSEs against the sample sizes for the five parameter combinations, respectively.

6. Applications

This section demonstrates the applicability and effectiveness of the proposed NEGFFD using two real-world data sets. The performance of the NEGFFD is evaluated by comparing it with several competing models, namely: the Frechet Distribution (FD), Rayleigh Distribution (RD), Inverse Rayleigh Distribution (IRD), Inverse Weibull Distribution (IWD), Exponential Distribution (ED), and Inverse Lindley Distribution (ILD). The density functions of the competing models are given here.

Novel Exponentiated G-Family Fréchet Distribution (NEGFFD) is given in equation (6).

Frechet Distribution (FD) is given by in equation (3).

Rayleigh Distribution

$$f(x;\theta) = \frac{x}{\theta^2}\exp\left(-\frac{x^2}{2\theta^2}\right).$$

Exponential Distribution (ED)

$$f(x;\lambda) = \lambda\exp(-\lambda x).$$

Inverse Rayleigh Distribution (IRD)

$$f(x;\sigma) = \frac{2\sigma}{x^3}\exp\left(-\frac{\sigma}{x^2}\right).$$

Inverse Weibull Distribution (IWD)

$$f(x;\alpha,\beta) = \frac{\alpha}{\beta}\left(\frac{x}{\beta}\right)^{-(\alpha+1)}\exp\left(-\left(\frac{x}{\beta}\right)^{-\alpha}\right).$$

Inverse Lindley Distribution (ILD)

$$f(x;\theta) = \frac{\theta^2}{1+\theta}\cdot\frac{1+x}{x^3}\exp\left(-\frac{\theta}{x}\right).$$

To assess the adequacy of each model, we employ various model selection criteria, including the Akaike Information Criterion (AIC), Corrected Akaike Information Criterion (AICC), Bayesian Information Criterion (BIC), and Hannan–Quinn Information Criterion (HQIC). A lower value of these criteria indicates a better fit to the data. Additionally, the Kolmogorov–Smirnov (KS) statistic and its corresponding p-value were computed to assess the goodness-of-fit for each distribution.

Table 1. MLEs and MSE for the parameters α, β, and θ

Sample size	MLEs			Bias			MSE		
n	α	β	θ	α	β	θ	α	β	θ
Combination 1: $\alpha_0 = 0.5, \beta_0 = 0.5, \theta_0 = 1$									
25	0.51212	0.51619	1.20149	0.01212	0.01619	0.20149	0.06621	0.05797	0.97694
50	0.51019	0.51061	1.10819	0.01019	0.01061	0.10819	0.02566	0.02638	0.34154
100	0.50887	0.50929	1.0570	0.01019	0.01061	0.10819	0.02375	0.02334	0.24254
200	0.50930	0.49370	1.01680	0.0093	-0.0063	0.0168	0.00039	0.00035	0.00042
Combination 2: $\alpha_0 = 1.5, \beta_0 = 0.5, \theta_0 = 1$									
25	1.47580	0.52653	1.19300	-0.02420	0.02653	0.19300	0.13108	0.11019	1.47114
50	1.49400	0.51452	1.10784	-0.00600	0.01452	0.10784	0.06842	0.02793	0.35238
100	1.49756	0.50715	1.08726	-0.00244	0.00715	0.08726	0.05739	0.02629	0.29132
200	1.48623	0.50618	1.02347	-0.01377	0.00618	0.02347	0.00178	0.00083	0.00125
Combination 3: $\alpha_0 = 0.5, \beta_0 = 0.5, \theta_0 = 2$									
25	0.51507	0.51761	2.09552	0.01057	0.01761	0.09552	0.06300	0.10302	2.25097
50	0.51048	0.51254	2.06347	0.01048	0.51524	0.06347	0.02375	0.02629	0.59241
100	0.50911	0.50746	2.01801	0.00911	0.00746	0.10801	0.02227	0.02326	0.46997
200	0.49148	0.50972	2.02135	-0.00852	0.00972	0.02135	0.00328	0.00457	0.00141
Combination 4: $\alpha_0 = 3, \beta_0 = 5, \theta_0 = 2$									
25	2.85700	5.15348	2.14940	-0.143	0.15348	0.1494	1.15138	4.12044	1.25608
50	2.92784	5.08186	2.07182	-0.07216	0.08186	0.07182	0.27826	1.20192	0.45383
100	2.96152	5.01565	2.05681	0.03848	0.0155	0.05681	0.19891	0.78538	0.29318
200	2.98216	5.04257	2.01543	-0.01784	0.04257	0.01543	0.00674	0.00953	0.01081
Combination 5: $\alpha_0 = 3, \beta_0 = 1.5, \theta_0 = 2$									
25	2.86942	1.55765	2.19560	-0.13058	0.05765	0.1956	0.97972	0.45946	1.57194
50	2.92857	1.53300	2.08772	-0.07143	0.033	0.08772	0.28057	0.12812	0.51274
100	2.96148	1.51512	2.06604	-0.03852	0.01512	0.06604	0.19903	0.09039	0.32182
200	2.98671	1.50321	2.01543	-0.01329	0.00321	0.01329	0.01254	0.00763	0.01081

https://doi.org/10.57647/mathsci.2025.1904.17

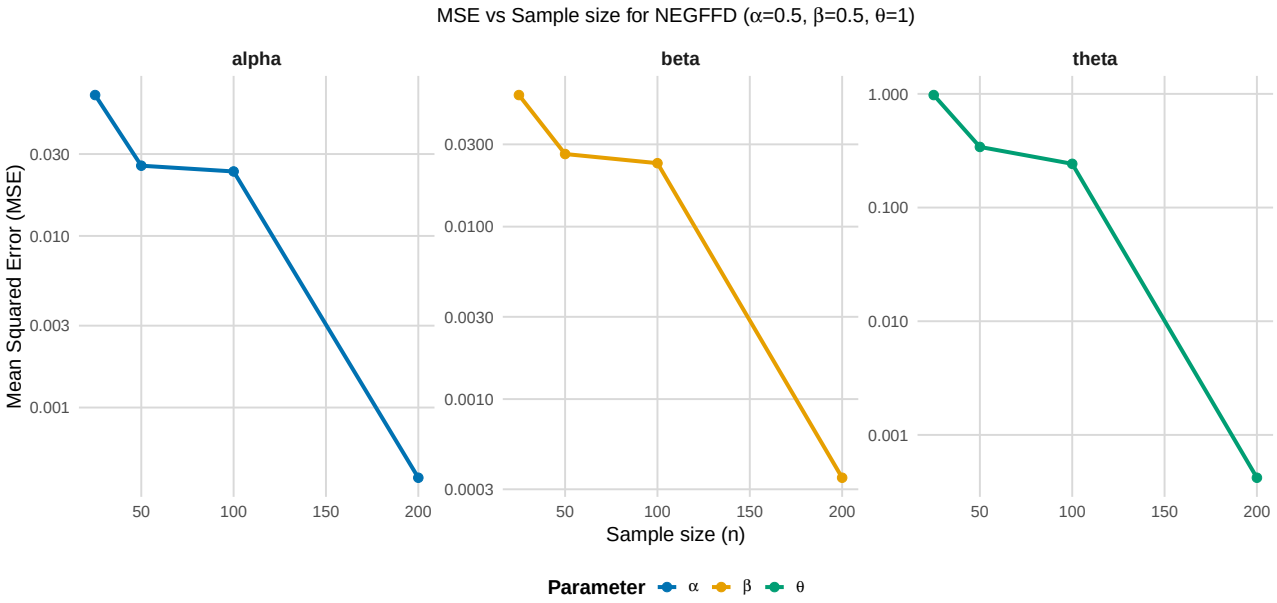

Figure 4. Plot of the MSE values against sample sizes for the NEGFFD model.

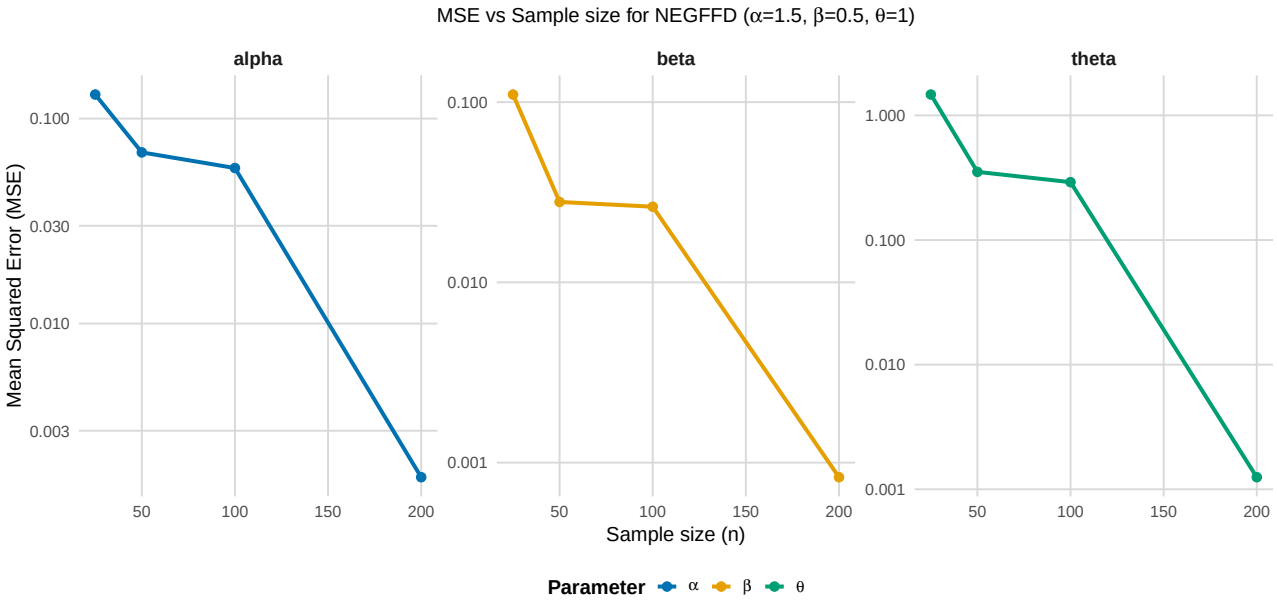

Figure 5. Plot of the MSE values against sample sizes for the NEGFFD model.

https://doi.org/10.57647/mathsci.2025.1904.17

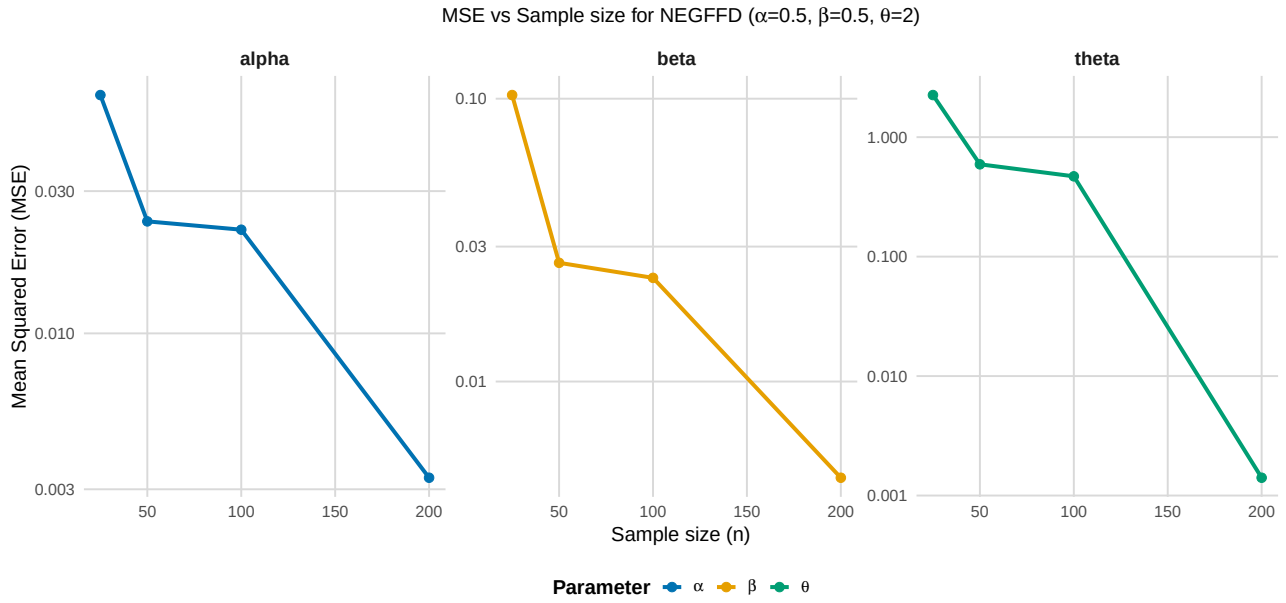

Figure 6. Plot of the MSE values against sample sizes for the NEGFFD model.

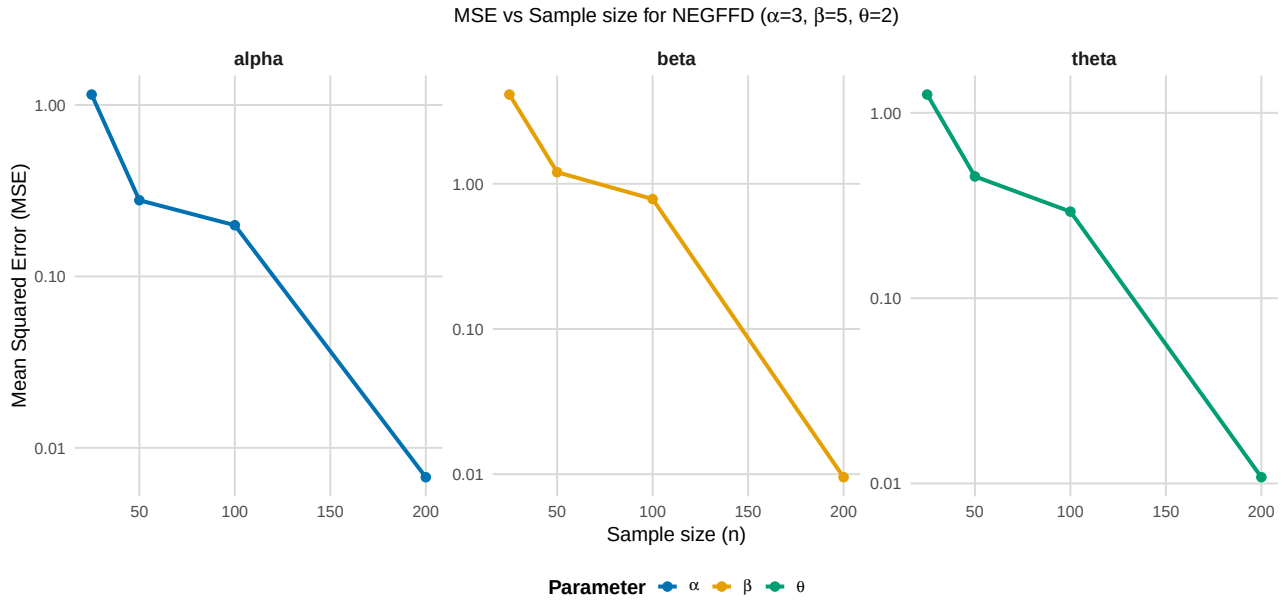

Figure 7. Plot of the MSE values against sample sizes for the NEGFFD model.

https://doi.org/10.57647/mathsci.2025.1904.17

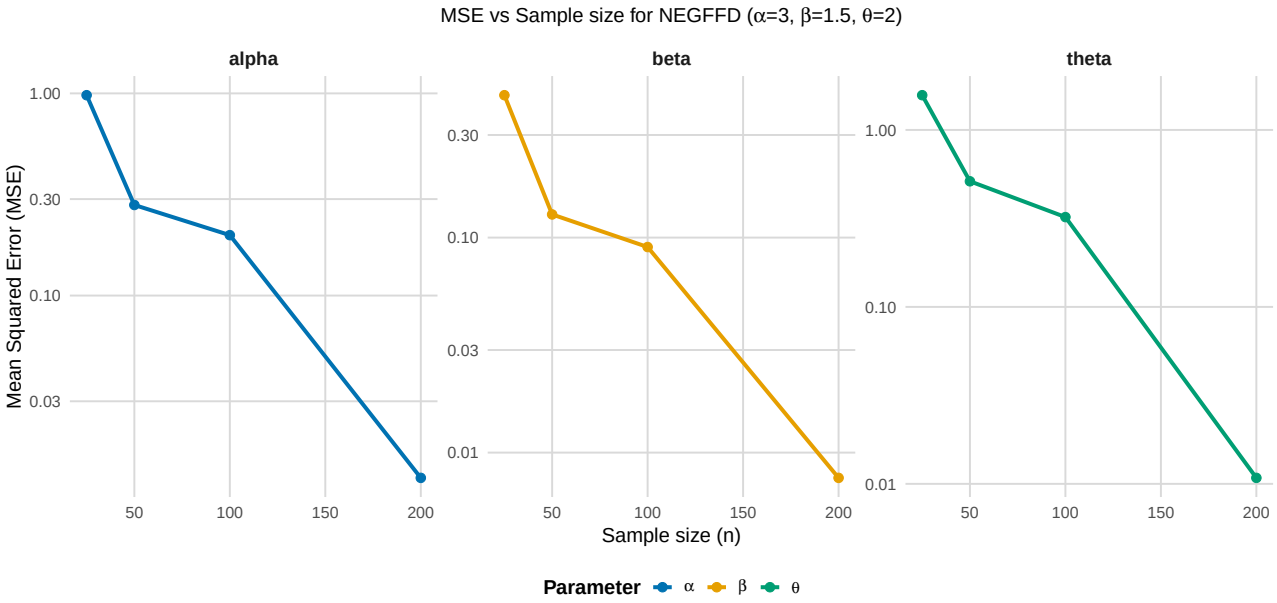

Figure 8. Plot of the MSE values against sample sizes for the NEGFFD model.

Table 2 and Table 4 present the MLEs, standard errors (SEs). Table 3 and Table 5 shows the associated fit statistics for all considered models. The NEGFFD consistently achieves the smallest values for $-2\log L$, AIC, AICC, BIC, and HQIC, along with the highest KS p-value and the lowest KS distance, thereby providing the best fit among the models considered. Figs. 9, 10, 11 and 12 represents graphically $-2\log L$, AIC, AICC, BIC, and HQIC, along with the highest KS p-value and the lowest KS distance. Figs. 13 , 14 and 15 illustrate the histogram of fitted density plots, and probability–probability (P–P) plots for the NEGFFD distribution based on the two datasets.The NEGFFD provides the best fit according to all considered statistical indicators.

6.1 Epidemiological data

This study uses an epidemiological dataset comprising COVID-19 death records reported in Canada between 10 April and 15 May 2020. The data were obtained from the World Health Organization (WHO) COVID-19 database (https://covid19.who.int/), which provides daily official statistics on confirmed cases and deaths as reported by national health authorities. This dataset was previously analysed by Almetwally et al. [15], who employed it to evaluate several statistical distributions for modelling COVID-19 mortality data. It was selected for the present study because it offers a practical example of skewed and heavy-tailed data, a characteristic commonly observed in epidemiological research. Owing to these properties, the dataset is particularly suitable for assessing the performance of the proposed NEGFFD in capturing skewed and heavy-tailed mortality patterns. These characteristics make the dataset particularly suitable for evaluating the performance of the proposed NEGFFD in capturing skewed and heavy-tailed mortality patterns.

The data are as follows: 3.1091 3.3825 3.1444 3.2135 2.4946 3.5146 4.9274 3.3769 6.8686 3.0914 4.9378 3.1091 3.2823 3.8594 4.0480 4.1685 3.6426 3.2110 2.8636 3.2218 2.9078 3.6346 2.7957 4.2781 4.2202 1.5157 2.6029 3.3592 2.8349 3.1348 2.5261 1.5806 2.7704 2.1901 2.4141 1.9048.

The statistical results for the epidemiological data are shown in Table 2 and Table 3.

6.2 Environmental data

This study uses an environmental dataset comprising March precipitation measurements (in inches) for Minneapolis and St. Paul, Minnesota, in the United States. The dataset was originally published by Hinkley (1977) in Applied Statistics as part of his research on power transformations. It was later analyzed by Alsadat et al. [16] to evaluate several statistical distributions for modeling precipitation patterns. The dataset consists of thirty continuous, positive observations representing variations in precipitation. The proposed NEGFFD was chosen for this study to assess its potential for modeling environmental processes. The data are as follows: 2.2, 3.37, 1.43, 0.74, 1.2, 1.95, 1.2, 0.81, 1.74, 0.77, 0.81, 0.59, 0.32, 1.31, 1.62, 0.52, 2.1, 1.51, 3.09, 3.00, 2.05, 0.9, 1.89, 0.96, 2.48, 4.75, 1.35, 1.18, 1.87, 2.81.

The statistical results for the environmental data are shown in Table 4 and Table 5.

7. Conclusion

This study introduced the NEGFFD framework, anchored by its Fréchet-based core form, a new three-parameter lifetime model that offers significant flexibility for modeling diverse data behaviors and versatile addition to statistical modeling. The proposed distribution serves as a unifying framework, generalizing the frechet distribution as a special case. A key feature of the NEGFFD is its highly adaptable hazard rate function, which can ef-

Table 2. MLEs (with standard errors) for different models for epidemiological data

Model	α	θ	β	λ	σ
NEGFFD	86.773 (125.418)	0.668 (0.209)	83.209 (123.397)	–	–
FD	–	3.169 (0.365)	2.704 (0.151)	–	–
RD	–	2.422 (0.201)	–	–	–
ED	–	–	–	0.3047 (0.0507)	–
IRD	–	–	–	–	8.2338 (1.3723)
IWD	3.1691 (0.3654)	–	2.7043 (0.1512)	–	–
ILD	–	3.6546 (0.5178)	–	–	–

Table 3. Goodness-of-fit statistics for different models for epidemiological data

Model	$-2l$	AIC	BIC	AICC	HQIC	K-S	p-value
NEGFFD	96.6287	102.6287	107.3793	103.3787	104.2868	0.11463	0.731
FD	105.8401	109.8401	113.0072	110.2038	110.9455	0.17376	0.2272
RD	116.9323	118.9323	120.5159	119.05	119.485	0.28023	0.007008
ED	177.273	159.5595	161.1431	159.6772	160.1122	0.4097	1.128×10^{-5}
IRD	171.917	119.7570	121.3405	119.8746	120.3097	0.28	0.008
IWD	105.8401	109.8401	113.0072	110.2038	110.9455	0.17376	0.2272
ILD	156.0879	158.088	159.6715	158.2056	158.6406	0.41932	6.352×10^{-6}

Table 4. MLEs (standard errors) for different models for environmental data

Model	α	θ	β	λ	σ
NEGFFD	40.4427 (48.9130)	0.3658 (0.1053)	334.4033 (802.5117)	–	–
FD	–	1.5966 (0.2064)	1.0446 (0.1269)	–	–
ED	–	–	–	0.5938 (0.1084)	–
IRD	–	–	–	–	0.93074 (0.16992)
IWD	1.5966 (0.2064)	–	1.0446 (0.1269)	–	–
ILD	–	1.6244 (0.2332)	–	–	–

Table 5. Goodness-of-fit statistics for different models for environmental data

Model	$-2l$	AIC	BIC	AICC	HQIC	K-S	p-value
NEGFFD	78.6299	84.6299	88.8335	85.5530	85.9747	0.0806	0.9899
FD	82.6628	86.6628	89.4652	87.1073	87.5594	0.1390	0.6080
ED	91.2703	93.2703	94.6715	93.4131	93.7185	0.2556	0.0400
IRD	86.1686	88.1686	89.5698	88.3114	88.6168	0.2125	0.1331
IWD	82.6628	86.6628	89.4652	87.1073	87.5594	0.1390	0.6080
ILD	90.3387	92.3387	93.7399	92.4816	92.7870	0.2357	0.0713

https://doi.org/10.57647/mathsci.2025.1904.17

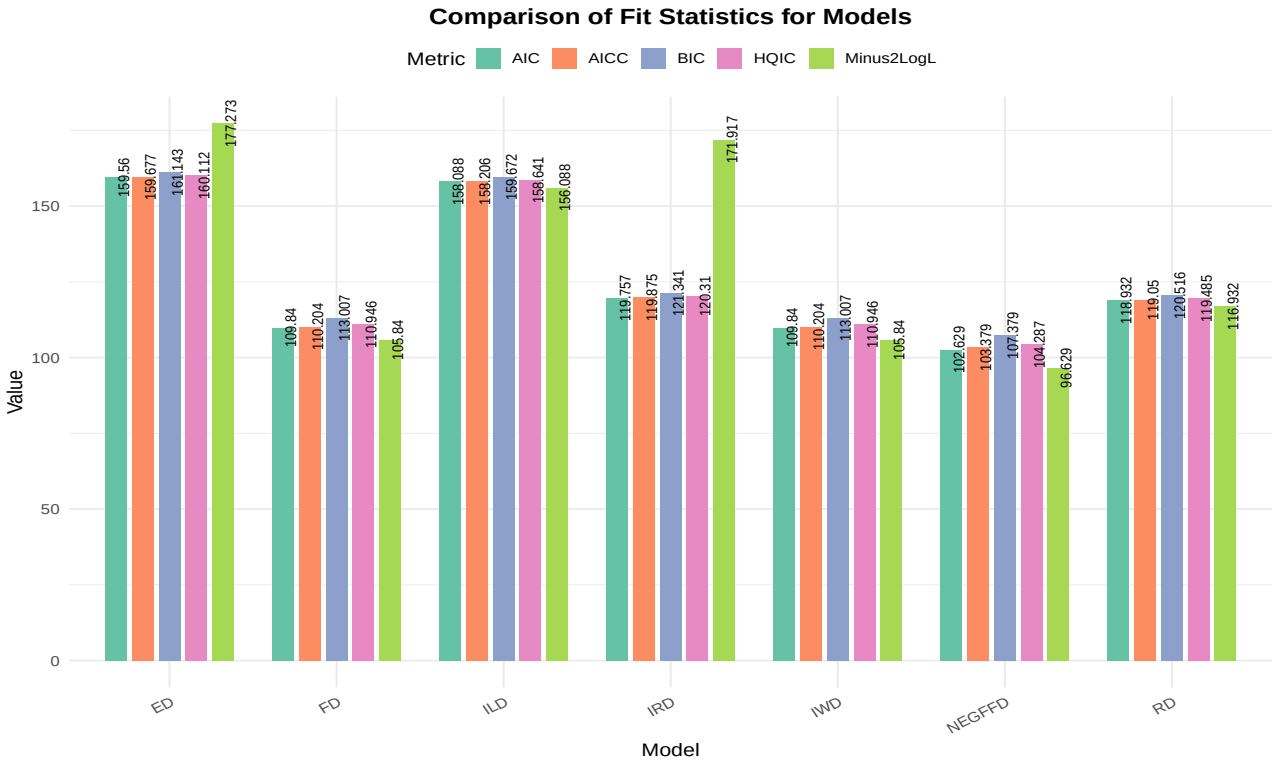

Figure 9. Plotting of the results given in Table 3 for epidemiological data

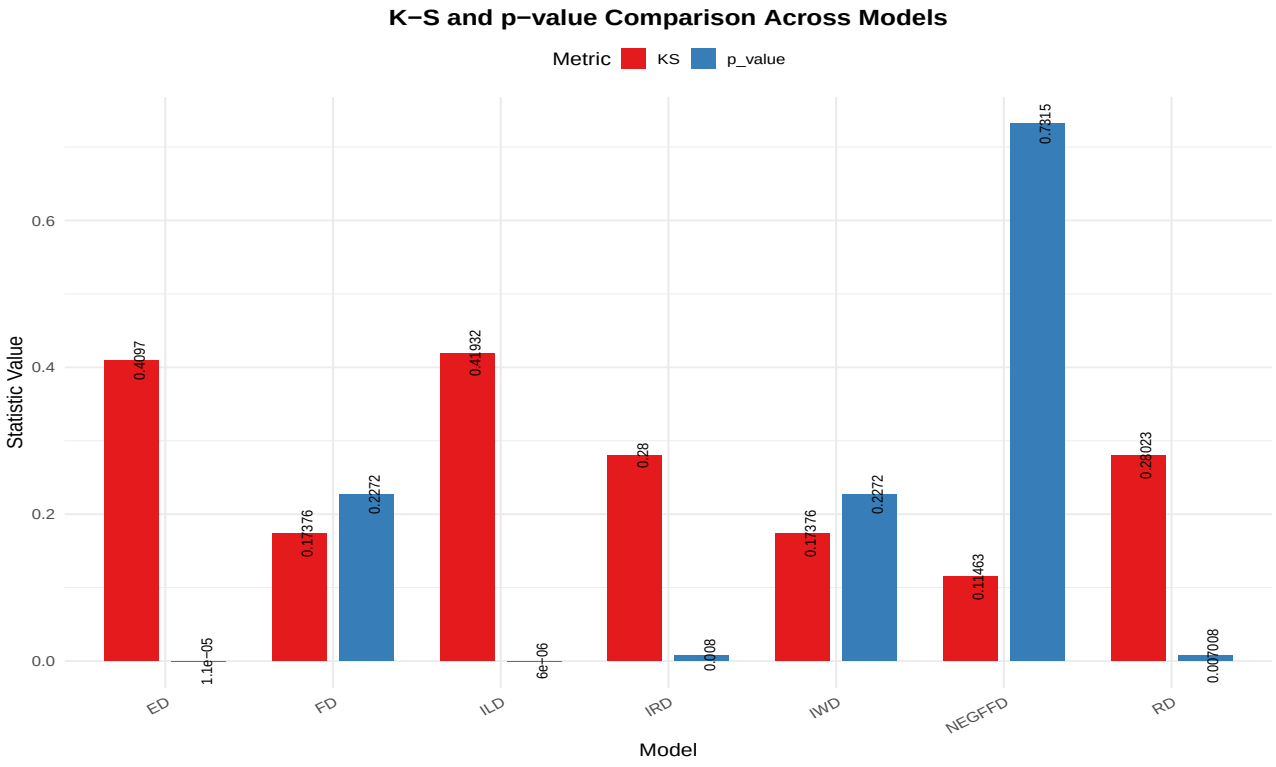

Figure 10. Plotting of the k-S and p-value given in Table 3 for epidemiological data

https://doi.org/10.57647/mathsci.2025.1904.17

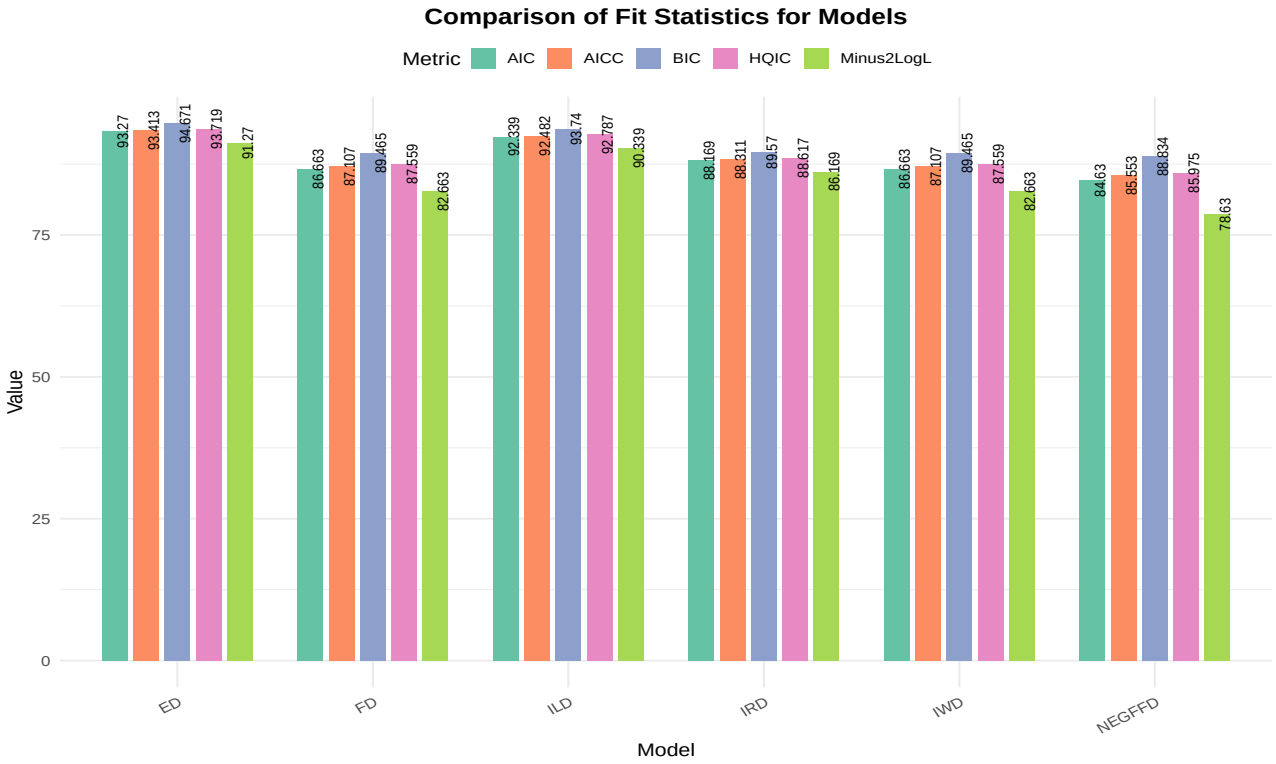

Figure 11. Plotting of the results given in Table 5 for environmental data

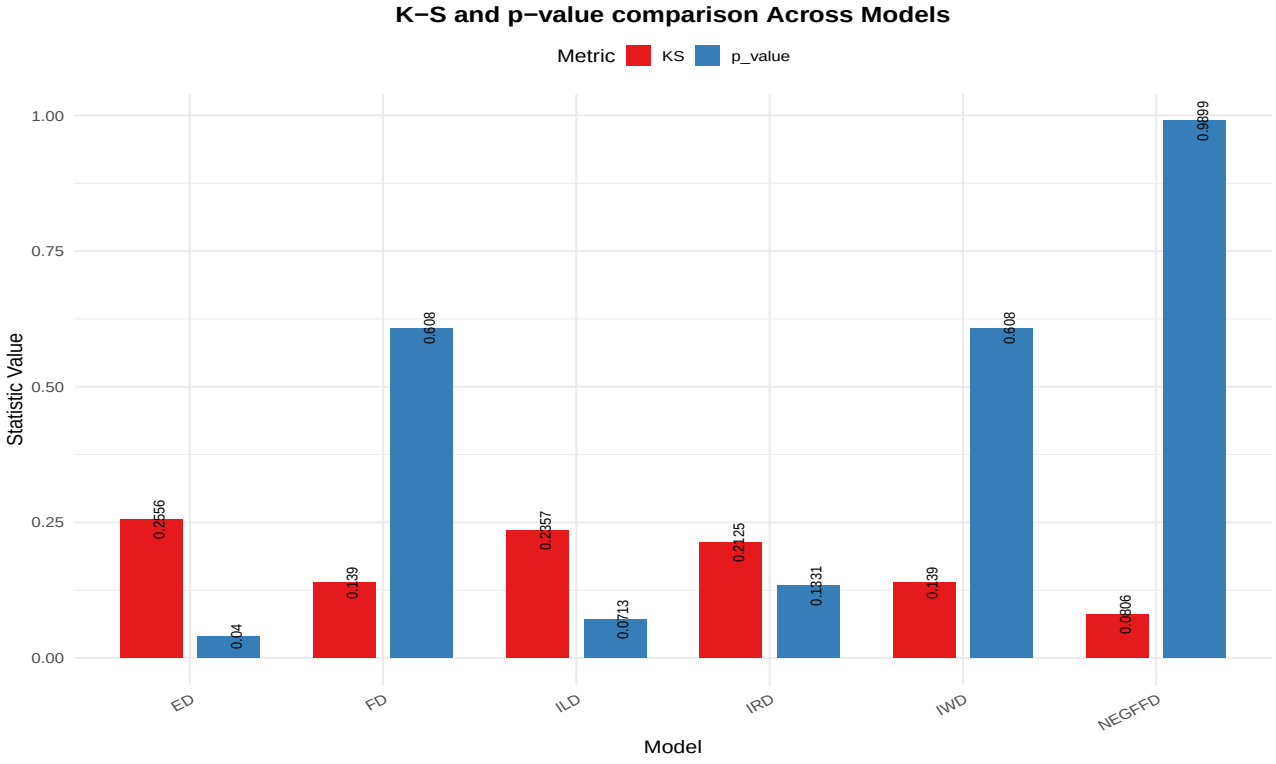

Figure 12. Plotting of the k-S and p-value given in Table 5 for environmental data

https://doi.org/10.57647/mathsci.2025.1904.17

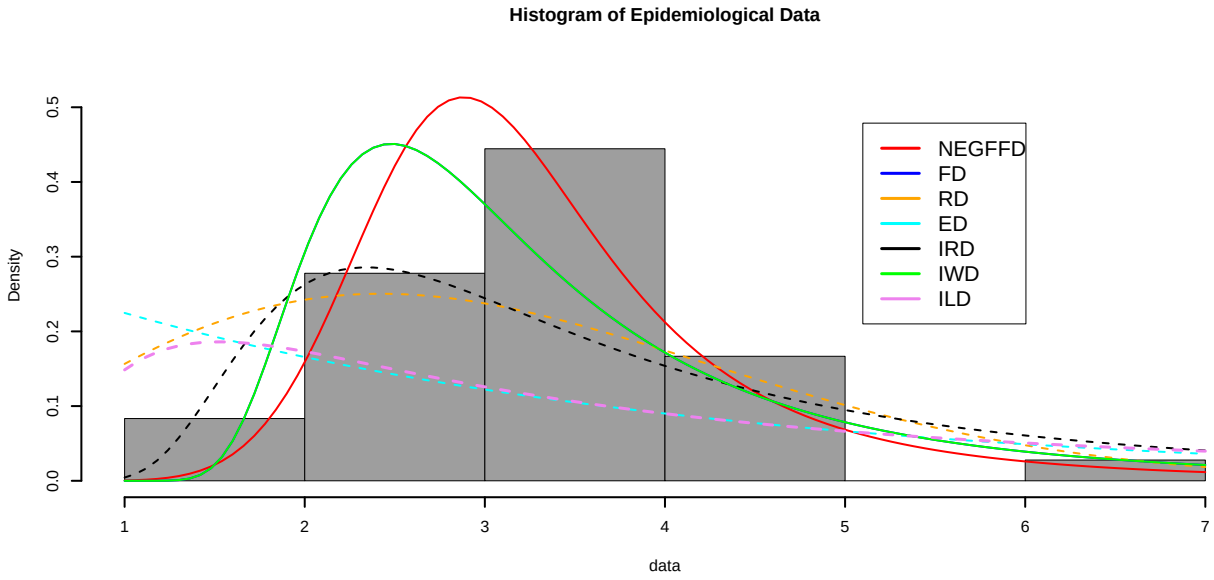

Figure 13. Fitted density plot for epidemiological data

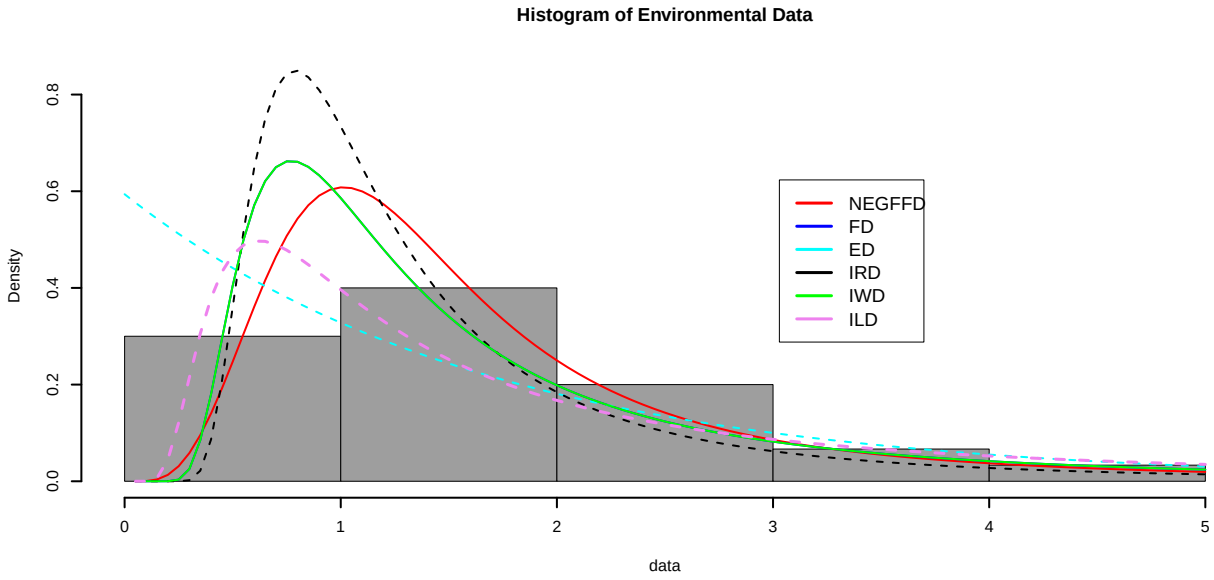

Figure 14. Fitted density plot for environmental data

https://doi.org/10.57647/mathsci.2025.1904.17

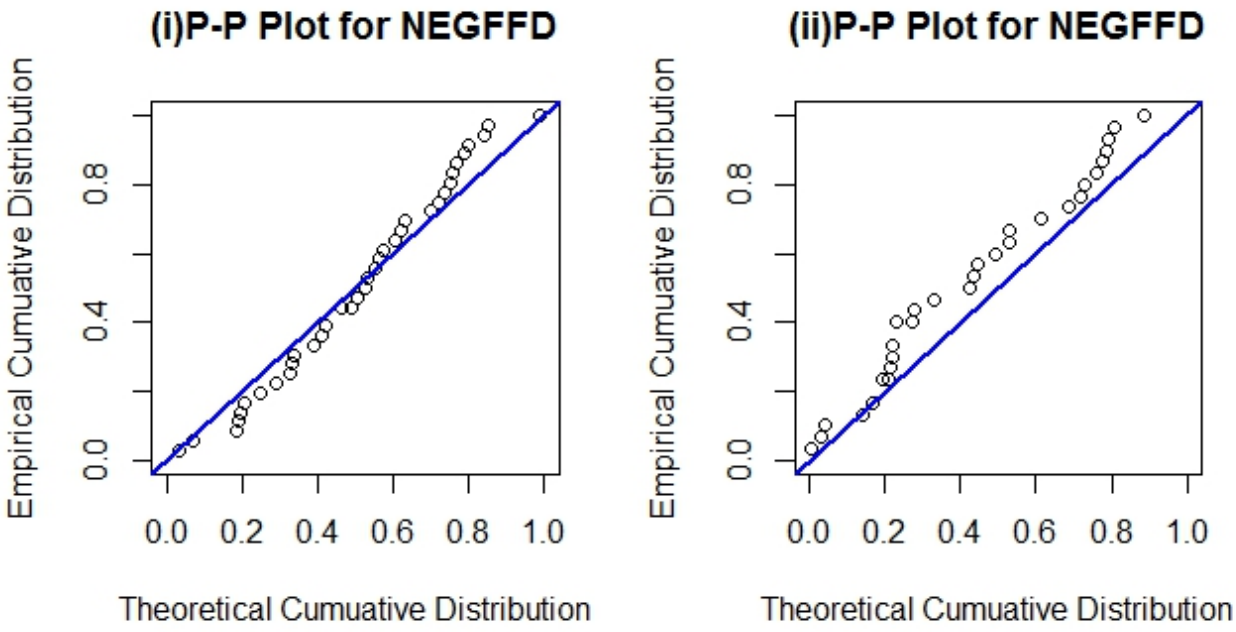

Figure 15. P-P Plot of NEGFFD for epidemiological data and environmental data

fectively capture increasing, decreasing, bathtub-shaped, and upside-down bathtub (unimodal) failure patterns, making it a robust tool for reliability and survival analysis. A comprehensive mathematical treatment of the model was provided. We derived several essential structural properties in closed form such as a series expansion of the probability density function, the quantile function, moments, mean deviations, order statistics, entropy measures, mean residual life, mean waiting time, order statistics. For parameter estimation, the MLE was used. Theoretical developments have established the comprehensive mathematical foundation of the NEGFFD, including the derivation of its probability density function, cumulative distribution function, hazard rate function, moments, and order statistics. These analytical results provide researchers with the necessary tools for parameter estimation and statistical inference.

Simulation studies demonstrated the robust performance of the model under varying parameter configurations.From simulation studies, it was observed that as the sample size increases , the MSE decreases and the MLEs increase closer to the true parameter values. The practical utility and superior performance of the NEGFFD were demonstrated conclusively through its application to simulation and two real-world datasets from different domains. In all cases, the proposed model provided an excellent fit to the data, outperforming its nested sub-models and other competing distributions. This empirical evidence strongly supports NEGFFD as a versatile and robust statistical tool. Its successful application across such disparate fields highlights a unique adaptability, suggesting that it is well-suited to the challenges of modern, interdisciplinary data analysis.

Looking ahead, the NEGFFD framework presents a fertile ground for future research. Promising directions include the development of extended models, perhaps incorporating additional shape parameters or Bayesian estimation techniques, to enhance flexibility and inference. Furthermore, applying this framework to novel challenges in fields such as economics, engineering, and computational biology will provide a more extensive assessment of its limits and solidify its position as a valuable asset in the statistician's toolkit.

Acknowledgment

This study is supported via funding from Prince Sattam bin Abdulaziz University project number (PSAU/2025/R/1447).

Authors contributions
All the authors have participated sufficiently in the intellectual content, conception and design of this work or the analysis and interpretation of the data (when applicable), as well as the writing of the manuscript.

Availability of data and materials
The data supporting the findings of this study are available within the article.

Conflict of interests
The authors declare that there are no conflict of interest.

References

1. Coles S, Bawa J, Trenner L, and Dorazio P. An introduction to statistical modeling of extreme values. Vol. 208. Springer, 2001
2. Fréchet M. Sur la loi de probabilité de l'écart maximum. Ann. de la Soc. Polonaise de Math. 1927
3. Mudholkar GS and Srivastava DK. Exponentiated Weibull family for analyzing bathtub failure-rate data. IEEE transactions on reliability 1993; 42:299–302
4. Marshall AW and Olkin I. A new method for adding a parameter to a family of distributions with application to the exponential and Weibull families. Biometrika 1997; 84:641–52
5. Odhah OH, Alshanbari HM, Ahmad Z, Khan F, and El-Bagoury AAH. A new family of distributions using a trigonometric function: Properties and applications in the healthcare sector. Heliyon 2024; 10
6. Shah Z, Khan DM, Khan I, Ahmad B, Jeridi M, and Al-Marzouki S. A novel flexible exponent power-X family of distributions with applications to COVID-19 mortality rate in Mexico and Canada. Scientific Reports 2024; 14:8992
7. Alzaatreh A, Lee C, and Famoye F. A new method for generating families of continuous distributions. Metron 2013; 71:63–79
8. Kumar D, Singh U, and Singh SK. A new distribution using sine function-its application to bladder cancer patients data. Journal of Statistics Applications & Probability 2015; 4:417
9. Mir AA, Rasool SU, Ahmad S, Bhat A, Jawa TM, Sayed-Ahmed N, and Tolba AH. A robust framework for probability distribution generation: Analyzing structural properties and applications in engineering and medicine. Axioms 2025; 14:281
10. Rasool SU, Lone M, and Ahmad S. An innovative technique for generating probability distributions: A study on lomax distribution with applications in medical and engineering fields. Annals of Data Science 2025; 12:439–55
11. Farooq M, Ali M, Zaman Q, et al. EXPONENT BETA FRECHET DISTRIBUTION AND ITS APPLICATIONS TO MEDICAL AND ENGINEERING SCIENCES. Journal for Current Sign 2025; 3:1–12
12. Igiozee M, Afolabi JM, and Ehigie O. On development of exponentiated frechet weibull distribution: properties and applications. Frontline Professionals Journal 2025; 2:35–46
13. Tzavelas G, Batsidis A, and Economou P. Size Biased Fréchet Distribution: Properties and Statistical Inference. Journal of Statistical Theory and Applications 2024; 23:456–79
14. Rényi A. On measures of entropy and information. *Proceedings of the Fourth Berkeley Symposium on Mathematical Statistics and Probability, Volume 1: Contributions to the Theory of Statistics*. Vol. 4. University of California Press. 1961 :547–62
15. Almetwally EM, Alharbi R, Alnagar D, and Hafez EH. A new inverted topp-leone distribution: applications to the COVID-19 mortality rate in two different countries. Axioms 2021; 10:25
16. Alsadat N, Ahmad A, Jallal M, Gemeay AM, Meraou MA, Hussam E, Elmetwally EM, and Hossain MM. The novel Kumaraswamy power Frechet distribution with data analysis related to diverse scientific areas. Alexandria engineering journal 2023; 70:651–64